Supporting Information

UBC9 mutant reveals the impact of protein dynamics on substrate selectivity and SUMO chain linkages

Christine M. Wright[†#], Robert H. Whitaker[‡#], Joshua E. Onuiri[†#], Tessa Blackburn[‡], Sierra McGarity[†], Mary-Ann Bjornsti[†*], and William J. Placzek[‡*]

[†]Department of Pharmacology and Toxicology, and [‡]Department of Biochemistry and Molecular Genetics, The University of Alabama at Birmingham, Birmingham, Alabama.

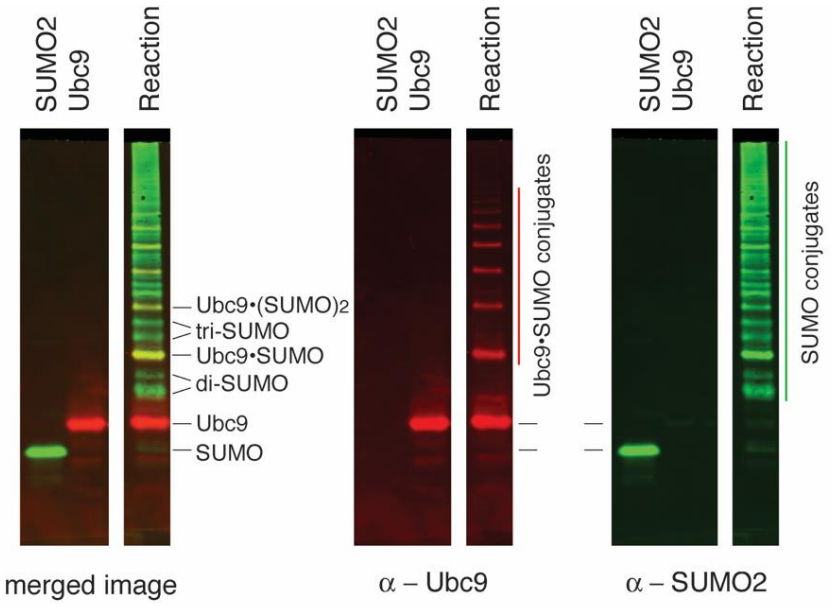

Figure S1. ***In vitro*** **SUMOylation assay with human UBC9 and SUMO-2**. Purified human E1, UBC9 (E2) and SUMO-2 (molar ratio of 1:2.5:3, respectively) were incubated with ATP at 37˚C for 2 hours. Following DDT treatment, to resolve SUMO-2 thioester linkages with the active cysteines of the E1 and UBC9, the reaction products were resolved by 4-12% Bis-Tris SDS-PAGE (ThermoFisher) and transferred to FL-PVDF membranes. The use of infrared fluorescence, IRDye secondary antibodies and Odyssey imaging (LI-COR) allowed for simultaneous staining with mouse anti-UBC9 antibody (BD Biosciences) and rabbit anti-SUMO2+3 antibody (Abcam). Subsequent incubation with secondary antibodies [goat anti-rabbit IRDye 800CW and goat anti-mouse IRDye 680 (LI-COR)] allowed for direct visualization of UBC9 containing bands at 800nm (red channel) and SUMO2 containing bands (green), respectively. Overlay of pseudo colored UBC9 and SUMO bands (merged image) are in yellow. Purified SUMO-2 and UBC9 proteins were included as controls. This representative image is from n>10.

In the presence of ATP and the E1 enzyme, Lys residues in UBC9 and SUMO-2 themselves serve as substrates for isopeptide bond formation between the C-terminal di-Gly end of mature SUMO-2 with the ε-amine of the acceptor Lys. In SUMO-2, K11 is contained within a consensus site motif in the unstructured N-terminus and is the major SUMOylation site (see Fig. 1). However, SUMOylation of nonconsensus site residues (K5,7 in the extended N-terminus) and K42,45 residues embedded in an alpha-helical structure have been reported. The detection of two di-SUMO isoforms (and higher SUMO conjugates) suggest the formation of distinct SUMO chain linkages, which produce altered electrophoretic mobilities in the SDS PAGE system used in these studies. UBC9•SUMO indicates isopetide bond linkage of SUMO-2 to UBC9, preferentially at K14. Consequently, higher order UBC9 conjugates may reflect chains at K14, modification of other Lys residues, or a combination of both. The thioester linkage of SUMO-2 to the active site cysteine of UBC9, which precedes conjugation and is resolved by DTT, is indicated by UBC9~SUMO in other figures.

Knipscheer P., Flotho A., Klug H., Olsen J. V., van Dijk W. J., Fish A., Johnson E. S., Mann M., Sixma T. K., Pichler A. (2008) Mol. Cell 31, 371–382

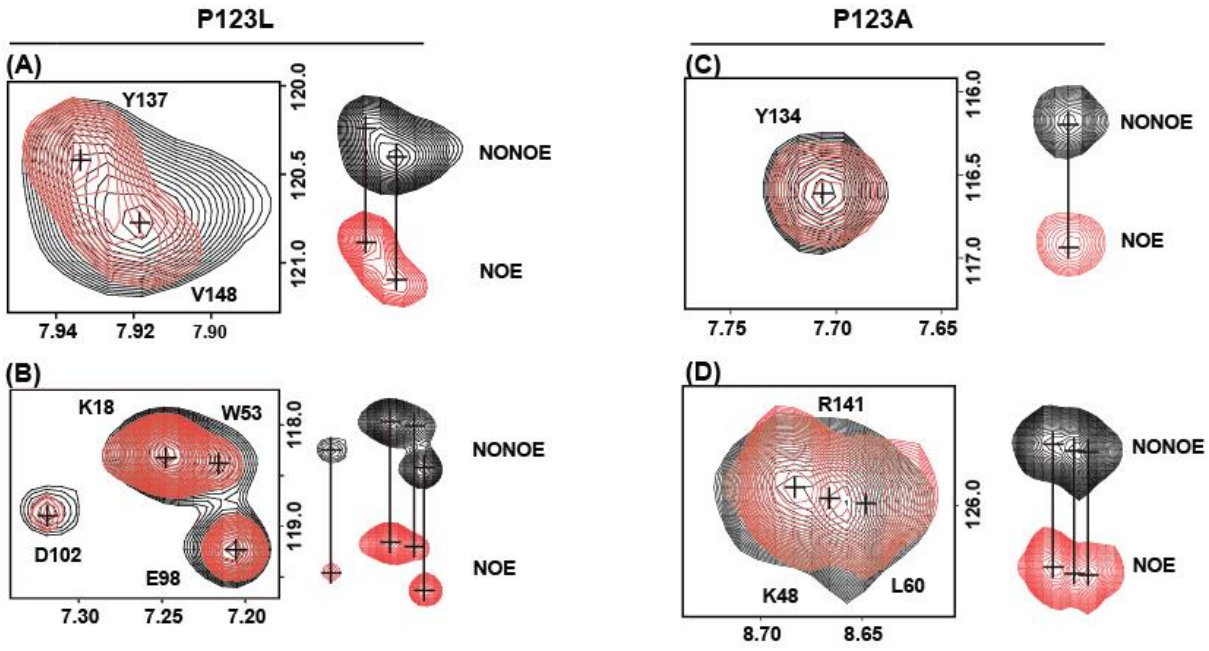

Figure S2. Representative ^{15}N-{^{1}H} NOE crosspeaks from P123L and P123A spectra. Overlay of select crosspeaks from the NONOE (black) and ^{15}N-{^{1}H} NOE (red) spectra for: (A) representative residues in P123L (Y137 and V148) near the residues E132, Y134, and R141 that display single peaks in the NOE spectra of P123L; (B) additional representative P123L residual heteronuclear NOE crosspeaks; (C) the peaks arising from Y134 in P123A demonstrates a single chemical conformation in both NONOE and NOE; (D) a cluster of peaks in P123A, including the crosspeak arising from R141.

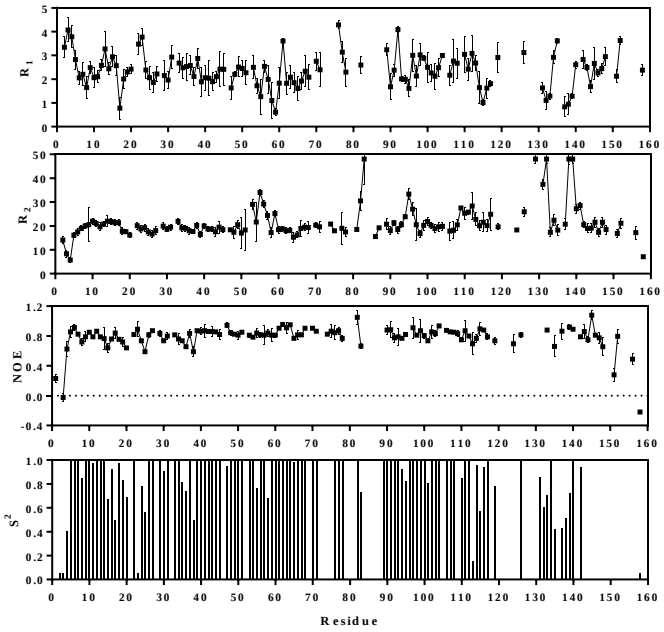

Figure S3. ^{15}N backbone dynamic analysis of P123L. Composite plots of R_1, R_2, NOE, and S^2. S^2 values were calculated in RotDif 3.1.

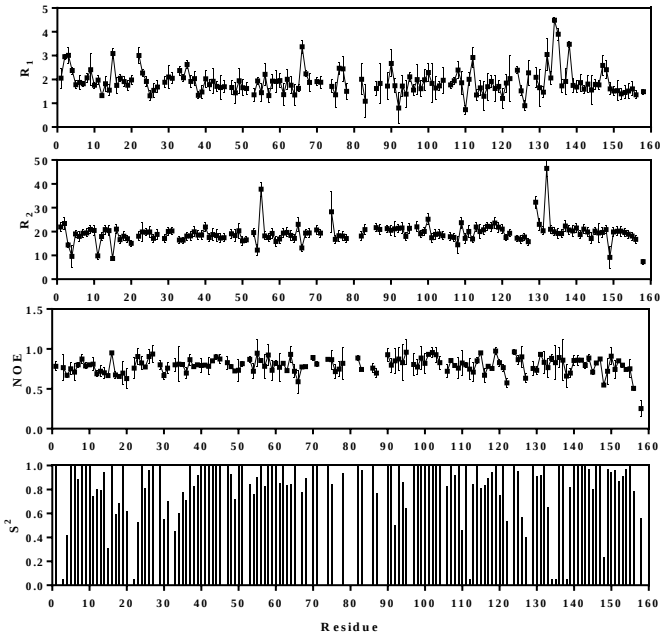

Figure S4. ^{15}N backbone dynamic analysis of P123A. Composite plots of R_1, R_2, NOE, and S^2. S^2 values were calculated in RotDif 3.1.

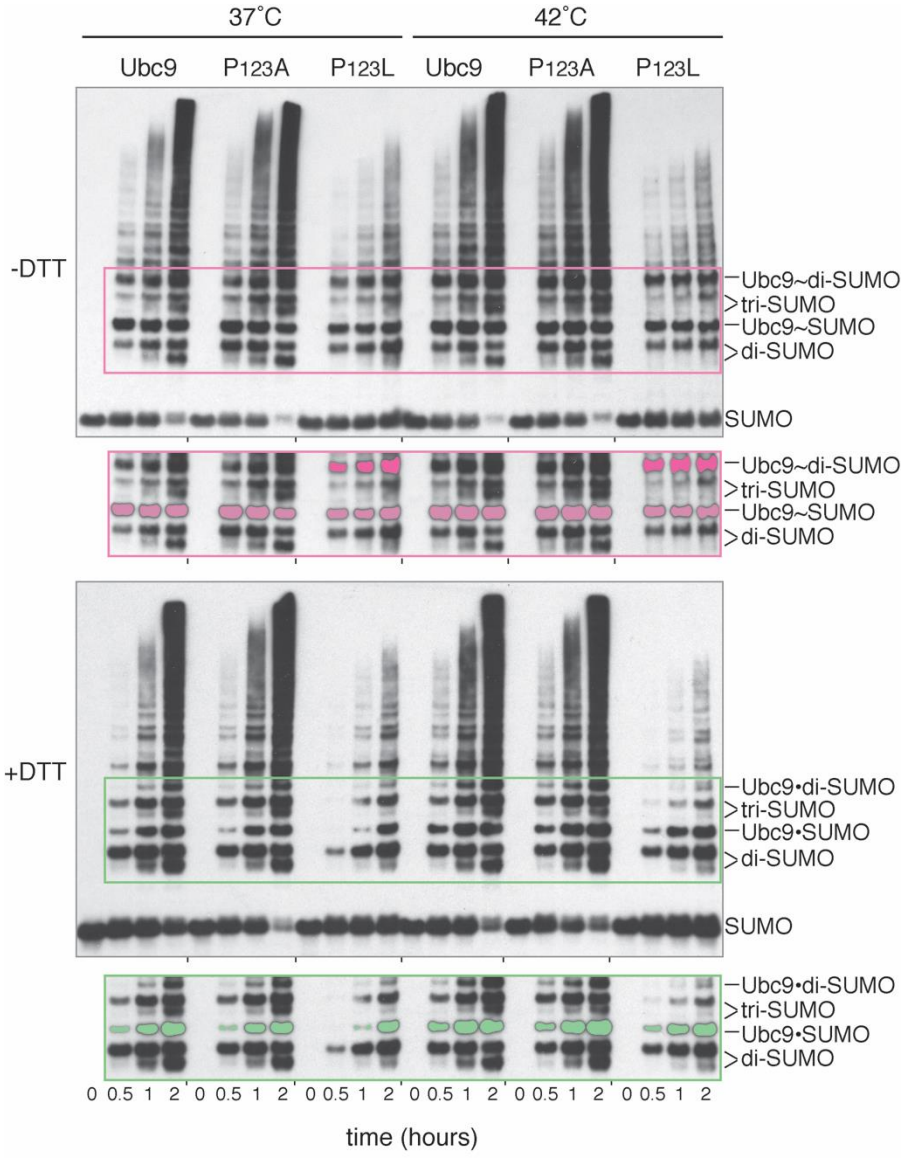

Figure S5. Thioester bond formation (loading of SUMO onto the active site cysteine of UBC9) is not impaired by the P123L mutation. During SUMOylation, the formation of a thioester linkage occurs between the carboxy terminus of SUMO and the active site cysteine of UBC9. This reaction intermediate (UBC9~SUMO) results from a transthiolation, whereby SUMO is transferred from the active site cysteine of the E1 to that of UBC9, and is required for the subsequent chemistry of SUMO isopeptide bond formation between SUMO and the acceptor Lys in the substrate protein. To assess whether the alterations in P123L catalysis results from impaired formation of UBC9~SUMO, a time course of SUMO conjugation was performed under reaction conditions described in Figure 7A and Figure S1. However, half of the reactions were treated with DTT and resolved by SDS-PAGE (+DTT), while the other half of each reaction was treated with sample buffer and resolved in SDS-polyacrylamide gels that lacked DTT (-DTT). The SUMO-2 –containing bands were then visualized by immunoblotting with anti-SUMO-2/3 antibodies from Abcam. The relative mobilities of di-SUMO, tri-SUMO, UBC9•SUMO (and di-SUMO) and UBC9~SUMO (and di-SUMO) are indicated. Image exposures of each blot were chosen to highlight alterations in the relative intensities of these bands (from n=3). In the case of –DTT samples, the UBC9~SUMO (or ~di-SUMO) bands also

include UBC9•SUMO (or •di-SUMO), as these species are not electrophoretically resolved. In the sections of the –DTT and +DTT blots delineated by the pink and green boxes, pseudo coloring of UBC9~SUMO (light pink) for all –DTT reactions, UBC9~di-SUMO (dark pink) for the P123L reactions at 37 and 42˚C, and UBC9•SUMO (green) for all +DTT reactions was done in photoshop and reproduced below each image to ease band identification and comparison.

In contrast to the time dependent increase in UBC9•SUMO observed with all reactions at 37˚C and 42˚C in the +DTT samples (in green), relatively constant levels of UBC9~SUMO are detected at all time points for each –DTT UBC9 protein (wild-type, P123A and P123L) at both temperatures (in light pink). These data suggest that the efficient loading of SUMO onto the active site cysteine of UBC9 is not impaired by P123L. Moreover, although there is a significant reduction in the relative amounts of UBC9•di-SUMO in the +DTT treated P123L samples, relative to wild-type UBC9 and P123A at both temperatures, the formation of UBC9~di-SUMO by P123L in the –DTT samples was not impaired (dark pink). UBC9~di-SUMO comprised of UBC9•SUMO loaded with a single SUMO, or unmodified UBC9 loaded with a di-SUMO chain cannot be distinguished in these analyses.

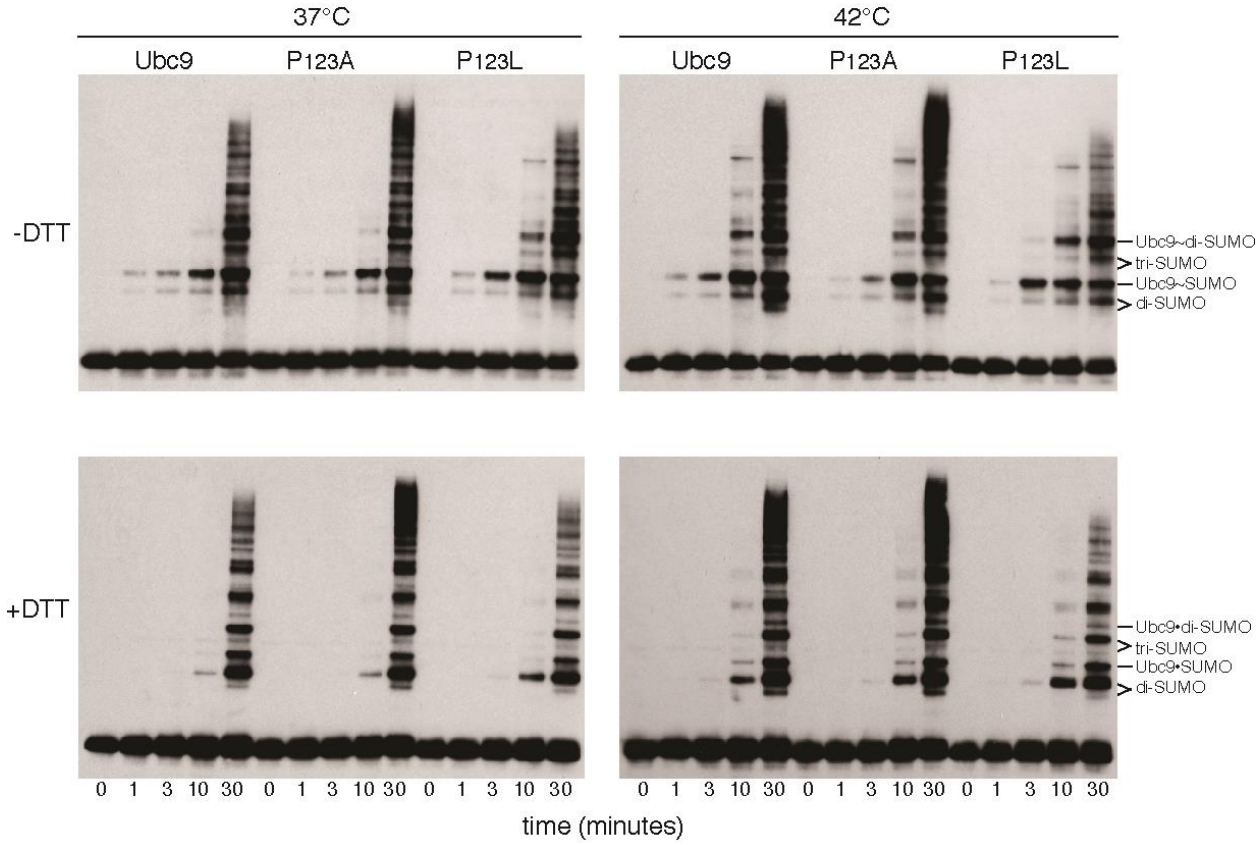

Figure S6. Thioester bond formation (loading of SUMO onto the active site cysteine of UBC9) is not impaired by the P123L mutation. Reactions carried out as in Supplementary Figure S5, over a shorter time frame. Shown is a representative figure of n=3. As in (A), no defect in the formation of UBC9~SUMO or UBC9~di-SUMO reaction intermediates was detected with P123L, in comparison with wild-type UBC9 or P123A, at 37˚C or at 42˚C in the –DTT samples. Moreover, in the +DTT P123L samples, the accumulation of UBC9•SUMO and the upper di-SUMO band, which involves SUMO conjugation of non-consensus SUMO sites, mirrored that of UBC9 and P123A at both temperatures. In contrast, a temperature sensitive decrease in the formation of the lower di-SUMO band, UBC9•di-SUMO and longer SUMO chains was evident with P123L at 42˚C.

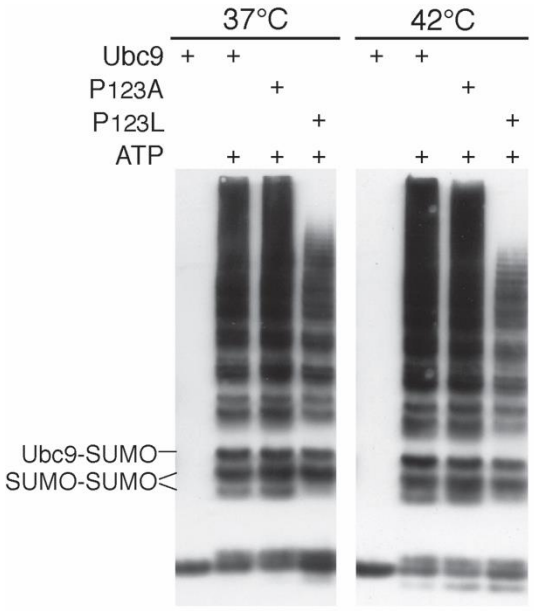

Figure S7. **P123L induces a switch in SUMO-1 chain linkage formation**. As described for SUMO-2 (see Figure 7A), purified human E1, UBC9 (wild-type, P123A or P123L) and SUMO-1 (molar ratio of 1:2.5:10, respectively) and ATP were incubated at 37˚C or 42˚C for 2 hours. The samples were treated with DTT, resolved by SDS-PAGE and blotted onto PVDF membranes. Following incubation with anti-SUMO-1 antibodies (Cell Signaling Technology), the SUMO-1 bands were visualized with SuperSignal West Dura (Thermo Fisher). As seen with SUMO-2, wild-type UBC9, and P123A efficiently catalyzed the formation of distinct di-SUMO isoforms (labeled SUMO-SUMO), UBC9•SUMO and higher order conjugates at both temperatures. Although SUMO-1 lacks consensus SUMO sites, the P123L reactions exhibited significantly lower levels of the lower di-SUMO band and higher order conjugates. These effects were more pronounced at the higher temperature of 42˚C. (n=3)

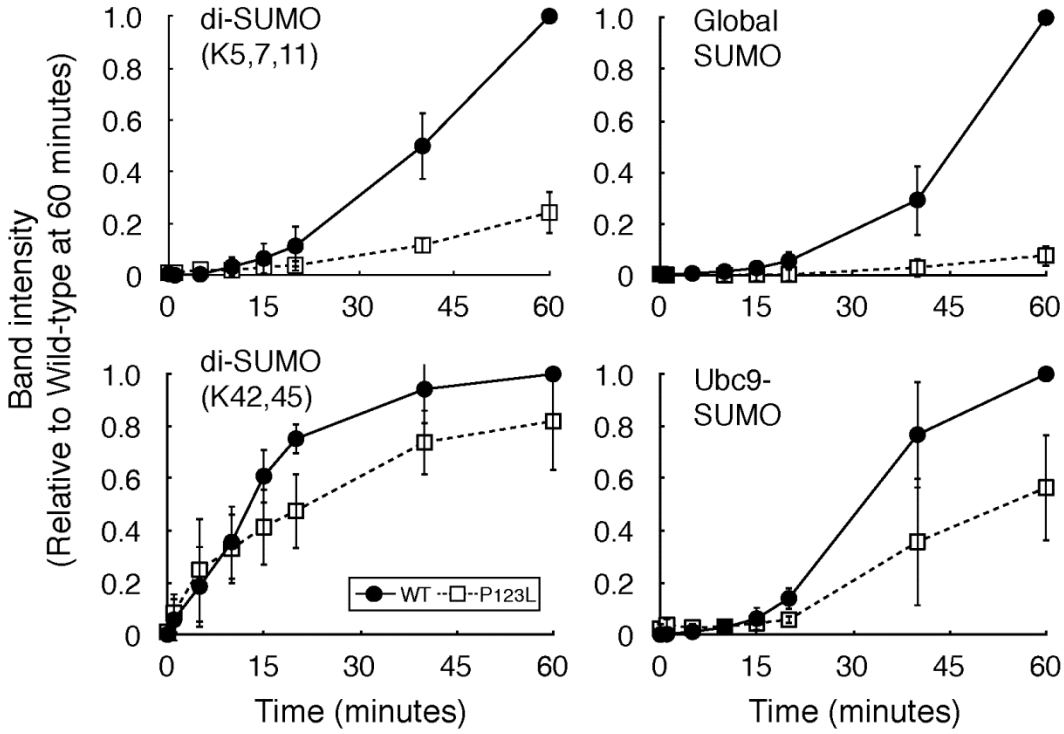

Figure S8. **A decrease in global SUMO conjugation and N-terminal SUMO chain linkage formation by P123L is also evident at 37˚C.** As described for P123L and wild-type UBC9 at 42˚C in Fig. 8B, the quantification of di-SUMO (K42, 45) versus di-SUMO (K5,7,11) band formation (n=3 independent experiments) indicate a P123L-induced switch in substrate preference from Lys residues in the extended N-terminus of SUMO2 to Lys residues in α-helical secondary structures. This effect was also mirrored in the relatively efficient formation of UBC9•SUMO conjugates by P123L, but a dramatic decrease in global SUMO conjugates as a consequence of decreased di-SUMO (K5,7,11) chain formation.